HHS Public Access

Author manuscript

Nat Cell Biol. Author manuscript; available in PMC 2014 May 01.

Published in final edited form as:

Nat Cell Biol. 2013 November ; 15(11): 1351–1361. doi:10.1038/ncb2861.

TGFβ2 dictates disseminated tumour cell fate in target organs through TGFβ-RIII and p38α/β signalling

Paloma Bragado[1], **Yeriel Estrada**[1], **Falguni Parikh**[1], **Sarah Krause**[2], **Carla Capobianco**[3], **Hernan G. Farina**[3], **Denis M Schewe**[1,2], and **Julio A. Aguirre-Ghiso**[1,4,5]

[1]Division of Hematology and Oncology, Department of Medicine, Department of Otolaryngology, Tisch Cancer Institute

[2]Department of General Pediatrics, University Hospital of Schleswig-Holstein, Kiel, Germany

[3]Laboratory of Molecular Oncology, Department of Science and Technology, Quilmes National University, Buenos Aires, Argentina

[4]Black Family Stem Cell Institute, Mount Sinai School of Medicine

Abstract

In patients non-proliferative disseminated tumour cells (DTCs) can persist in the bone marrow (BM) while other organs (i.e. lung) present growing metastasis. This suggested that the BM might be a metastasis "restrictive soil" by encoding dormancy-inducing cues in DTCs. Here we show in a HNSCC model that strong and specific TGFβ2 signalling in the BM activates p38α/β, inducing a $[ERK/p38]^{low}$ signalling ratio. This results in induction of *DEC2/SHARP1* and p27, downregulation of CDK4 and dormancy of malignant DTCs. TGFβ2-induced dormancy required TGFβ-receptor-I, TGFβ-receptor-III and SMAD1/5 activation to induce p27. In lungs, a metastasis "permissive soil" with low TGFβ2 levels, DTC dormancy was short lived and followed by metastatic growth. Importantly, systemic inhibition of TGFβ-receptor-I or p38α/β activities awakened dormant DTCs fueling multi-organ metastasis. Our work reveals a "seed and soil" mechanism where TGFβ2 and TGFβRIII signalling through p38α/β regulates DTC dormancy and defines restrictive (BM) and -permissive (lung) microenvironments for HNSCC metastasis.

Keywords

DTC; quiescence; target organ; seed and soil; metastasis

[5]*Correspondence to:* Julio A. Aguirre-Ghiso, Division of Hematology and Oncology, Department of Medicine, Mount Sinai School of Medicine, New York, NY, 10029. Phone: 212-241-9582 Fax: 212-241-4096 Box: 1079 julio.aguirre-ghiso@mssm.edu.

AUTHOR CONTRIBUTION: Conceived and designed the experiments: PB, YE, DS, HF, JA-G. Performed the experiments: PB, YE, FP, SK, CC, JA-G. Analyzed the data: PB, DS, HF, JA-G. Contributed reagents / Materials / analysis tools: DS, HF. Wrote the paper: PB, JA-G.

INTRODUCTION

The “seed and soil” theory of metastasis proposes that the fate of disseminated tumour cells (DTCs) is dependent on the microenvironment where they lodge[1]. This supports the organ-specific preference for metastasis in certain cancers. However, their timing is largely unpredictable because residual DTCs may be dormant for long periods[2,3]. Solitary bone marrow (BM) DTCs that are mostly negative for proliferation markers have been catalogued as in a cellular dormancy state functionally defined by quiescence[2]. Intriguingly, in many malignancies, while 30–40% of patients have BM DTCs, these rarely develop bone metastases (HNSCC, gastric cancer) or develop very late (breast cancer)[4,5]. A similar scenario for seed and soil mechanisms can be studied in mouse tumour models. While spontaneous metastases vigorously develop lungs and lymph nodes and, less frequently in liver[6], DTCs can be found in the BM and other sites in a non-productive state, at least in the same time frame[2,7]. Importantly, even in syngeneic models spontaneous overt bone lesions rarely develop, unless the microenvironment is altered[7]. This suggests that specific micro-environmental signals could keep DTCs dormant[5].

We reported a “dormancy gene signature” regulated by p38α/β kinase signalling in quiescent HNSCC cells[8]. Estrogen receptor (ER) positive luminal breast cancer tumours that were enriched for the dormancy signature displayed longer metastasis-free periods, suggesting that these dormancy genes in DTCs may affect metastasis timing[9]. Some of these genes (e.g. NR2F1[10], DEC2/SHARP1[11], FOXM1[12]) regulate pluripotency, predict for delayed recurrence in breast and prostate cancer[11], and suppress the malignant behaviour[8, 11]. Another signature gene, TGFβ2, was the most upregulated TGFβ-family cytokine in quiescent HNSCC cells *in vivo*. TGFβ2 can activate p38[13], induce quiescence and both these genes limit self-renewal[10,14]. Thus, we hypothesized that TGFβ2^{high} microenvironments might drive DTC dormancy. Here we reveal a previously unrecognized “seed and soil” mechanism where TGFβ2 signalling through p38α/β regulates DTC dormancy and defines restrictive (BM) and -permissive (lung) microenvironments for HNSCC metastasis.

RESULTS

The Bone Marrow Microenvironment Induces DTC Dormancy

HEp3-GFP cells obtained from xenografts were injected subcutaneously (s.c.) in nude mice and when primary tumours reached ~500 mm^3 (t0) they were surgically removed. Then, HEp3 spontaneous DTCs were followed using GFP fluorescence and by human *Alu* sequence-specific qPCR[15] to identify DTCs undetectable via GFP, or CK8/18 staining. This revealed a DTC prevalence of ~80% in lungs, ~28% in the BM and ~5% in liver and spleen at the time of dissection (Fig. 1a, Supplementary Table S1, Fig S1a–d). GFP+ cells imaged in fresh tissues *in situ*, were intact viable cells as determined by confocal imaging of DTCs *in situ* (Fig. 1a). In the BM the number of DTCs (GFP+) ranged from 10–10^2/BM, was >2 logs lower than in lungs (Fig. 1a, b, Supplementary Fig. S1a, c, d) and remained constant for at least 4 weeks after primary tumour surgery (Fig. 1b). In contrast, lung DTCs that were already present in the lung as single solitary cells at the time of surgery (Supplementary Fig. S1e), initiated vigorous proliferation 2 weeks after surgery (Fig. 1b).

In 100% of the cases we could expand *in vitro* HEp3 GFP-tagged DTCs (Puro-resistant) isolated from lungs (Lu-HEp3) and this was independent of the initial number of recovered lung DTCs (Supplementary Table S2). In stark contrast, in the ~28% of mice that had BM DTCs, while all these DTCs (BM-HEp3) survived plating, only 2/15 (13.3%) expanded in culture. The lack of proliferative capacity was persistent as evidenced by 86.6% of all BM DTC isolates resulting in GFP+ puromycin resistant solitary growth-arrested HEp3 DTCs for > 4 weeks in culture (Supplementary Table S2).

That ~86% of BM DTCs (Supplementary Table S2) are viable but non-proliferative in culture led us to hypothesize that the BM microenvironment may instruct DTCs to activate long-lasting dormancy programs. We could only study mechanistically those BM DTCs that expanded *in vitro* and focused on BM vs. lung derived DTCs because of their most divergent *in vivo* behaviour and clinical relevance[16] (Fig. 1a). We defined dormant DTCs as non-proliferating or slow-cycling cells, negative/low for proliferation markers (i.e. phospho-H3 (P-H3)) and positive/high for CDK inhibitor expression (i.e. p21, $p27^{Cip}$). Two lung (Lu-HEp3), two BM (BM-HEp3) and two primary tumour (PT-HEp3) derived cell lines, were screened for tumorigenicity in the chorioallantoic membrane (CAM) system[17–19] or in nude mice[8]. In all cases Lu-HEp3 and PT-HEp3 cells were tumorigenic and were P-$H3^{high}$/$p27^{low}$ (Fig. 1c, 1d, Supplementary Fig. S1f). In contrast, one BM-HEp3 cell line remained dormant for 4–5 weeks before growing vigorously (henceforth BM-D1) (Fig. 1e, Supplementary Fig. S1g); dormant BM-D1 cells were P-$H3^{low}$/$p27^{High}$ (Fig. 1d, Supplementary Fig. S1f), confirming their quiescent phenotype. Another BM derived DTC line (BM-T1) that did not proliferate in situ, fully reversed to a proliferative behaviour in culture and *in vivo* (Fig. 1c). In the nude mouse s.c., BM-D1 cells also formed tumours later than BM-T1 cells (Supplementary Fig. S1h). This data suggest that while ~85% of DTCs from murine BM will remain dormant and non-proliferative in culture half of those BM-DTCs that do expand in culture can retain a dormant phenotype when re-injected *in vivo* (Fig 1c–e).

We also obtained BM-DTCs cell lines from the chicken and turkey embryos BM because we could process larger numbers of animals and increase our chances of obtaining BM DTC lines (Supplementary Fig. S1i). DTCs were non-proliferative in avian BM but did proliferate in the liver and lungs where metastases develop[20] (Supplementary Fig. S1j). As in mice, the number of DTC in the BM was 2 logs lower than in the liver and lungs (Supplementary Fig. S1j). Importantly, 7/9 (77%) BM-DTC cell lines remained dormant *in vivo* (Fig. 1f- and Supplementary Fig S1k). We conclude that while 100% of lung derived DTC lines were tumorigenic, 13/15 (86.6%) of the BM-isolated DTCs were non-proliferative *in vitro* (up to 4–8- weeks) and 1/15 (~7%) was dormant *in vivo* after 5–6 weeks. Together, 14/15 (~93.3%) BM-derived DTCs from mice and 77% of BM-derived DTC lines in the avian system are dormant *in vitro* and/or *in vivo*. Thus, dormancy is the predominant phenotype of murine or avian BM-isolated human HNSCC DTCs.

Signalling Pathways Activated in Bone Marrow Dormant DTCS

We next measured previously identified key regulators of dormancy[8,21]. Proliferative Lu-HEp3 and BM-T1 cells from the murine system and BM-T2 and BM-T3 cells from the avian system displayed a high ERK/p38 ratio, consistent with their tumorigenicity. In contrast, the

dormant BM-D1 and BM-D2, D3, and D4 cells from murine and avian BM, respectively, displayed persistently low ERK/p38 activity ratio (Fig. 2a, 2b); BM-D5 was the only avian BM DTC line in which the ERK/p38 activity ratio (high) was not predictive of dormancy (Fig. 2b). The ERK/p38 ratio correlated also with the metastatic (4T1 and F3II[22] - [ERK/p38]^{high}) or dormant (4T07- [ERK/p38]^{low}) behaviour of mouse breast cancer cell lines in lungs[23] (Fig. S2a). Thus, a high ERK/p38 signalling ratio, (see Methods for quantification) is predictive of tumorigenic and dormant phenotype in 100% (n=9) and 90% (n=9) of the DTC lines, respectively (Fig. 2c). BM-D1 cells also up-regulated p53 (mRNA and protein) and DEC2 mRNA, two genes previously linked to dormancy and quiescence[8], when compared to the proliferative variants (Lu-HEp3 and BM-T1) cells. The p53 transcript was almost undetectable in 4T1, 4T07 and F3II cell lines, but DEC2 was vigorously upregulated in 4T07 vs. F3II and 4T1 metastatic cells (Fig. 2d, Supplementary Fig. S2b, c).

Knockdown of p38α, DEC2 or p53 interrupted the dormancy of BM-D1 cells (Fig. 2e, Supplementary Fig S2d) and sustained knockdown of DEC2 for two weeks allowed BM-D1 cells to completely regain tumorigenicity *in vivo*. This correlated with upregulation of CDK4 and inhibition of p27 (Fig 2f). Accordingly, overexpression of a constitutively active p38α (p38α-CA) mutant or wt-DEC2 cDNAs in proliferative Lu-HEp3 cells reduced P-H3 levels, did not affect apoptosis and inhibited their *in vivo* proliferation (Fig. 2f, Supplementary Fig. S2e, S2f); DEC2 overexpression in T-HEp3 cells also induced p27 and p21 expression while inhibiting CDK4 expression (Fig 2g). Analysis of human HNSCC primary and metastatic lesions showed that compared to normal oral epithelium, and stromal cells, in 4/4 patients, DEC2 protein was strongly downregulated in the primary tumours and also in the matched lymph node metastasis (Supplementary Fig. S2g). These results suggest that primary tumour and metastatic growth is associated with downregulation of DEC2 as a possible dormancy escape mechanism.

Systemic p38α/β inhibition fuels Occult DTC Expansion

Next we used the small molecule inhibitor SB203580 that faithfully phenocopies the genetic inhibition of at least p38α[8,19,21,24] to systemically inhibit p38α/β activity and test DTC fate after primary tumour surgery. We defined liver, spleen and BM as metastasis restrictive sites in nude mice because DTCs are detectable (Supplementary table S1) but never grow. Direct analysis of BM DTCs using cytokeratin 8/18 (CK) staining[7], showed that 80% were p27^{high}, only 1% were P-H3+ (Fig. 3a) supporting their dormant phenotype. Importantly, we found that after 4 weeks, SB203580 treatment significantly increased the prevalence and number of DTCs in the BM as detected by GFP imaging, *Alu* sequence specific qPCR or quantification of CK8/18 positive DTCs (Supplementary table S3, Fig. 3b). While the three different detection methods have limitations they all collectively support that p38α/β inhibition after surgery can increase the DTC burden in the BM. Similar results were observed in the liver and spleen where p38α/β inhibition for 4 weeks doubled the prevalence of DTCs, micro- and macro-metastasis in these organs (Supplementary table S3, Fig . 3c, 3d).

In the chick embryo system of metastasis[25] the liver and lung are permissive sites for metastasis[20,26]; liver DTCs (>10^5 cells/organ) are P-H3^{high}/p27^{low} and proliferate actively

(Supplementary Fig. S3a). The avian BM is also restrictive as DTCs (10^1–10^2 cells/BM) were also negative for P-H3 and positive for p27 (Supplementary Fig. S3a). After matching the primary tumours sizes (Supplementary Fig. S3b) we found that knockdown of p38α in T-HEp3 cells (siRNA knockdown can last for 5 days), increased the amount of DTCs in avian BM 5 days after inoculation (Fig 3e, Supplementary Fig. S3c). This increase correlated with a decrease in the percent of $p27^{high}$ DTCs, suggesting an exit from quiescence (Fig 3f). In the embryo liver (permissive site) p38α knockdown had no effect, possibly because DTCs grow immediately in this site (Supplementary Fig. S3d).

Solitary HEp3 lung DTCs identified by detecting human Vimentin (abundantly expressed in these cells - Supplementary Fig. S3e), were mostly negative for P-H3 and C-C3+, supporting that initially solitary lung DTCs are viable quiescent or slow-cycling tumour cells (Fig 4a, b). At 4 weeks, when macro-metastases are detectable and HEp3-GFP cell numbers raised in lungs, these lesions were $P\text{-}H3^{high}$ and $C\text{-}casp3^{low}$ (Fig 4a–c). Importantly, the p38α/β inhibitor treatment significantly increased HEp3-GFP HNSCC and F3II breast cancer metastatic cell burden after 2 and 4 weeks treatment (Fig. 4c, d). We conclude that p38α/β signalling limits the expansion of DTCs in growth-restrictive sites like mouse and chick embryo BM and in mouse liver and spleen. This effect is also observed on the short-term dormancy that solitary DTCs undergo in the lung in mice and the effect of p38α/β inhibition even on this short-term dormancy phase has a dramatic impact on disease burden in this tissue.

TGFβ2 Signalling in the BM Induces Dormancy Hallmarks

Expression profiling of proliferating (T-HEp3 [$ERK/p38^{high}$]) and dormant D-HEp3 ([$ERK/p38^{low}$]) cells *in vivo* revealed that TGFβ2 mRNA (not TGFβ1 or TGFβ3) is highly elevated only in dormant cells (Supplementary Fig. S4a). TGFβ2, which is present in the BM[27] activated p38, induced DEC2 and TGFβR-I-dependent quiescence in D-HEp3 cells (Supplementary Fig. S4b–d). In addition, dormant BM-D1 cells express >5-fold higher levels of TGFβ2 than parental T-HEp3 cells (T) and Lu-HEp3 cells (Fig. 5a). Importantly, we also found that TGFβ2 mRNA was greatly enriched in naÔve BM over lung tissue (Fig 5b) and that in basal conditions (serum free media) T-HEp3 cells express marginal TGFβ2 mRNA (Fig. 5a, c). Upon treatment of T-HEp3 cells with lung CM, TGFβ2 mRNA is increased. However, treatment with BM CM vigorously upregulated TGFβ2 expression (>10 fold - Fig. 5c), inhibited T-HEp3 tumour growth *in vivo* and this was positively correlated with upregulation of p27 and downregulation of P-H3 levels *in vivo* (Fig. 5d, e). In addition, the BM, but not lung CM, induced p38 phosphorylation and DEC2 and p53 mRNA expression in T-HEp3 and 4T1 cells (Fig. 5f, g and Supplementary Fig. S4e). Lung CM enhanced phospho-ERK1/2 levels (Fig 5f) and none of the organ-CM induced apoptosis (Supplementary Fig S4f). Importantly, TGFβ2-depleted BM CM was incapable of inducing p38 activation and growth inhibition of T-HEp3 cells *in vivo* (Fig. 5f, 5h) while lung CM supplemented with TGFβ2 inhibited T-HEp3 tumour growth *in vivo* (Fig. 5h). TGFβ2 depletion from BM CM did not restore ERK1/2 phosphorylation (see discussion) (Fig. 5f) and significantly, depletion of TGFβ1 from the BM CM, did not affect its ability to activate p38 or inhibit tumour growth (Supplementary Fig. S4g). In fact, treatment with TGFβ1, rapidly switched of dormant D-HEp3 and BM-D1 cells from dormancy to rapid tumour

growth *in vivo* while not affecting at all T-HEp3 tumorigenicity (Fig 5i). These data suggests that TGFβ2 but not TGFβ1 is a candidate mediator of p38 activation, DEC2 expression and dormancy in the BM.

We also found that the high basal p38 phosphorylation in BM-D1 cells was not stimulated by TGFβ2 treatment but was inhibited by LY-364947 suggesting maximally activated TGFβ-receptor signalling in these cells (Fig. 6a). TGFβ2 upregulated P-p38 and p21 levels in PT-HEp3, BM-T1 and T-HEp3 cells (Fig. 6a, b). Further, TGFβ2 induced DEC2 and/or p53 (not in the mouse lines) mRNAs in human HNSCC and mouse breast cancer metastatic cells while LY364947 treatment reduced their expression in BM-D1 and D-HEp3 cells (Fig. 6c, 6d, Supplementary Fig. S4c, S5a). Further, knockdown of TGFβ2 or the TGFβRI inhibitor interrupted the dormancy of BM-D1 cells (Fig. 6e, 6f, Supplementary Fig S5b). TGFβ2 also inhibited 4T1 tumour sphere formation (Supplementary Fig S5c), a measure of self-renewal that was linked to their metastatic capacity[28]. Similarly, treatment of the dormant 4T07 cells[28] with LY364947 or SB203580 enhanced tumour sphere formation or proliferation per tumour sphere (Supplementary Fig S5d, e). We conclude that dormancy of D-HEp3 and BM-D1 cells is dependent on TGFβ2, p38α/β, DEC2 and p53, which in turn induce p21, p27 and growth arrest. TGFβ2, TGFβRI and p38 signalling also appear to regulate self-renewal properties of breast cancer 4T07 cells that spontaneously enter solitary dormancy in lungs[28].

TGFβ-receptor-III regulates TGFβ2 signalling for dormancy

In analyzing the mechanism by which TGFβ1 and TGFβ2 signalling differs we found that at short time points (10 – 30 minutes) both TGFβ1 and TGFβ2 equally activate SMAD1/2/3/5 phosphorylation with no effect on SMAD4/6 total protein levels (Fig. 7a); at 2 hrs, TGFβ1 and TGFβ2 also showed a similar response, but now total SMAD3/4/6 were upregulated. However, we found that only TGFβ2 treatment induced a sustained phosphorylation of SMAD1/5, SMAD2 and to some extent SMAD3 at longer times (24h - Figure 7b). In addition, TGFβ2 but not TGFβ1 activated p38α, induced p27 and DEC2 expression and downregulated CDK4 at 24 hrs (Figure 7b–d). TGFβ2-induced SMAD2 phosphorylation and p27 upregulation was also inhibited by SB203580 (Figure 7e).

TGFβ2 requires the type III TGFβ receptor for signalling, while this receptor is dispensable for TGFβ1 signalling[29,30]. T-HEp3 cells express all three TGFβ-receptors *in vivo* (Supplementary Fig S5b) and RNAi to TGFβRIII had no significant effect on basal growth of these cells, but it completely eliminated the capacity of TGFβ2 to inhibit growth *in vivo* (Figure 7f, Supplementary Fig. S5c). This correlated with the inability of TGFβ2 to induce long-term SMAD1/5 phosphorylation and p27 induction in TGFβRIII^{low} cells (Figure 7g). TGFβRIII was not required for SMAD2 or p38 activation by TGFβ2 (Supplementary Fig. S5d). TGFβ1 did not stimulate T-HEp3 *in vivo* growth and TGFβRIII downregulation did not affect this lack of effect by TGFβ1 on these cells (F5i, 7h). We propose that TGFβRIII is required for the growth inhibitory function that TGFβ2 exerts on malignant HEp3 cells.

TGFβRI inhibition favours DTC escape from dormancy

While we found that TGFβ2 may prevents DTC expansion by inducing dormancy, TGFβ1 signalling can promote metastasis[31]. To determine how the apparently competing functions of TGFβ1 and TGFβ2 signalling affect DTC behaviour, we systemically inhibited TGFβ Receptor-I using LY-364947 and monitored DTC fate as in Fig3. Treatment with LY-364947 after primary tumour surgery approximately doubled the prevalence of spleen and liver DTCs (Figure 8a) and increased BM DTCs by ~5.6 fold (Fig. 8b). We also found that compared to control animals, treatment with LY-364947 increased the prevalence and the total metastatic burden in lungs by ~3-fold (Fig. 8c). These data support that in restrictive and permissive sites dormancy is a default state for DTCs and that signalling via TGFβRI (and possibly TGFβ2-TGFβRIII) might be at least in part responsible for the lack of DTC growth that is eliminated upon LY-364947 treatment.

DISCUSSION

We explored the mechanistic basis of microenvironment-driven DTCs dormancy, taking advantage of the HEp3 system of overt spontaneous metastasis, which in mice mimics that of HNSCC patients[32]. Despite their limitations, this model also mimics the presence of non-proliferative DTCs in the BM, as observed in HNSCC and breast cancer patients[3]. While our monitoring of DTC dormancy in the BM spanned 4 weeks, which is equivalent to ~3 years in humans, dormancy periods may span decades in patients. The fact that mice never develop over BM metastasis argues that monitoring DTCs in this site for longer periods may be an approximate model of the human situation. Our data suggests that BM DTCs undergoing prolonged dormancy display a set of markers (TGFβ2^{high}/[ERK/p38]^{low}/DEC2^{high}/p53^{high}/p27^{high}/P-H3^{low}) indicative of quiescence. 4T07 cells that enter dormancy in lungs when spontaneously disseminating[23] also displayed a dormancy profile ([ERK/p38]^{low}/DEC2^{high}) suggesting a metastasis-restrictive role for these pathways also in breast cancer cells. Our work now provides a set of microenvironment (e.g. TGFβ2) and DTCs markers ([ERK/p38]^{low}/DEC2^{high}, etc.) that may be potentially used to determine the proliferative vs. dormant state DTCs in BM or other sites. Undoubtedly, testing these markers in DTCs from patients with advanced or no evidence of disease, is key to fully validate our findings[33].

We found that at least TGFβ2 may define metastasis-restrictive vs. -permissive microenvironments. But other cues may also be important for BM DTC dormancy because TGFβ2 depletion from BM CM reduced p38 phosphorylation, but it did not activate ERK1/2. This could be due to the presence of BMP7, which induced a [ERK/38]^{low} ratio and prostate tumour cell dormancy in BM[34] or to other signals like the GAS6/Axl pathway[35] that also regulate dormancy and would have to be fully eliminated to restore a [ERK/p38]^{high} ratio and metastatic growth. In addition, higher TGFβ1 levels[36] or downregulation of TGFβRIII[37] may be needed to reprogram DTCs out of dormancy.

Our work also shows that TGFβ2, which due to its low affinity for TGFβRII, requires TGFβRIII[38,39], creates a unique signal that results in prolonged SMAD1/2/5 activation and p27 upregulation to induce quiescence. How TGFβ2 and TGFβ1 activate different signals is unclear but it may depend on the composition and/or activity of the TGFβRI/TGFβRII

complex[40] (Fig. 8d). Our results showing that TGFβ2 did not require TGFβRIII for p38 activation, further argues that different downstream complexes funnel the signals through the canonical (i.e. SMADs) and non-canonical (i.e. p38) pathways. Together, our data support that at least in HNSCC cells, TGFβ2 signalling through TGFβRI and TGFβRIII provides a qualitatively different signal from TGFβ1 to induce growth arrest. Because, TGFβRIII can activate p38 to induce growth arrest[41] and it can suppress tumorigenesis[42,37,43], it is possible that TGFβRIII^{high} DTCs may be more prone to enter dormancy in TGFβ2-rich microenvironments like the BM.

Our results using kinase inhibitors of p38α/β and TGFβRI support that both these kinases hold multi-organ residual disease from expanding into metastasis. The fact that lung DTCs proliferated after TGFβRI inhibition suggests that to some extent the TGFβ2-TGFβRIII-dependent dormancy is transiently operational and then reversed by opposing signals, perhaps TGFβ1. In this regard while TGFβ1 signalling has been linked to EMT and metastasis[31], a large body of work supports the growth suppressive function of TGFβ2 in normal and cancer cells[44,45]. Interestingly, the association of TGFβRIII loss with prostate bone metastasis development[46,47], suggests that TGFβRIII makes DTCs impervious to the TGFβ2 growth-suppressive signal in the BM. We propose that dormancy is an initial default program for DTCs and that TGFβ2 growth-suppressive function via TGFβR-I and -III might mediate these events. Other models and ours provide insight into the regulation of DTC biology. Validation in humans of our findings and those in other models[34,35,48] will further our understanding of DTC dormancy and aid the development of rational therapies to target dormant disease.

Supplementary Material

Refer to Web version on PubMed Central for supplementary material.

ACKNOWLEDGMENTS

Grant support: Samuel Waxman Cancer Research Foundation Tumour Dormancy Program, NCI CA109182 and CA163131, NIEHS (ES017146) and NYSTEM grants to J.A.A-G. Dr. Mildred-Scheel postdoctoral grant by the Deutsche Krebshilfe and Max-Eder Junior Research Grant by the Deutsche Krebshilfe e. V. to D.M.S. Carla Capobianco is a research fellow and Hernán Farina is an Investigator of CONICET - Argentina. This work was also supported by CONICET and UNQ grants to H.F.

REFERENCES

1. Fidler IJ. The pathogenesis of cancer metastasis: the 'seed and soil' hypothesis revisited. Nat Rev Cancer. 2003; 3:453–458. [PubMed: 12778135]
2. Aguirre-Ghiso JA. Models, mechanisms and clinical evidence for cancer dormancy. Nat Rev Cancer. 2007; 7:834–846. [PubMed: 17957189]
3. Klein CA. Framework models of tumor dormancy from patient-derived observations. Curr Opin Genet Dev. 2011; 21:42–49. [PubMed: 21145726]
4. Ferlito A, Shaha AR, Silver CE, Rinaldo A, Mondin V. Incidence and sites of distant metastases from head and neck cancer. ORL J Otorhinolaryngol Relat Spec. 2001; 63:202–207. [PubMed: 11408812]
5. Zhang Y, Ma B, Fan Q. Mechanisms of breast cancer bone metastasis. Cancer Letters. 2010; 292:1–7. [PubMed: 20006425]

6. Husemann Y, Klein CA. The analysis of metastasis in transgenic mouse models. Transgenic Res. 2009; 18:1–5. [PubMed: 19002597]
7. Husemann Y, et al. Systemic spread is an early step in breast cancer. Cancer Cell. 2008; 13:58–68. [PubMed: 18167340]
8. Adam AP, et al. Computational identification of a p38SAPK-regulated transcription factor network required for tumor cell quiescence. Cancer Res. 2009; 69:5664–5672. [PubMed: 19584293]
9. Kim RS, et al. Dormancy signatures and metastasis in estrogen receptor positive and negative breast cancer. PLoS One. 2012; 7:e35569. [PubMed: 22530051]
10. Onder TT, et al. Chromatin-modifying enzymes as modulators of reprogramming. Nature. 2012; 483:598–602. [PubMed: 22388813]
11. Montagner M, et al. SHARP1 suppresses breast cancer metastasis by promoting degradation of hypoxia-inducible factors. Nature. 2012; 487:380–384. [PubMed: 22801492]
12. Bao B, et al. Over-expression of FoxM1 leads to epithelial-mesenchymal transition and cancer stem cell phenotype in pancreatic cancer cells. J Cell Biochem. 2011; 112:2296–2306. [PubMed: 21503965]
13. Sorrentino A, et al. The type I TGF-beta receptor engages TRAF6 to activate TAK1 in a receptor kinase-independent manner. Nat Cell Biol. 2008; 10:1199–1207. [PubMed: 18758450]
14. Ito K, et al. Reactive oxygen species act through p38 MAPK to limit the lifespan of hematopoietic stem cells. Nat Med. 2006; 12:446–451. [PubMed: 16565722]
15. Zijlstra A, et al. A quantitative analysis of rate-limiting steps in the metastatic cascade using human-specific real-time polymerase chain reaction. Cancer Res. 2002; 62:7083–7092. [PubMed: 12460930]
16. Riethdorf S, Wikman H, Pantel K. Review: Biological relevance of disseminated tumor cells in cancer patients. International Journal of Cancer. 2008; 123:1991–2006.
17. Toolan HW. Transplantable Human Neoplasms Maintained in Cortisonetreated Laboratory Animals: H.S. #1; H.Ep. #1; H.Ep. #2; H.Ep. #3; H.Emb.Rh. #1. Cancer Research. 1954; 14:660–666. [PubMed: 13209540]
18. Ossowski L. Plasminogen activator dependent pathways in the dissemination of human tumor cells in the chick embryo. Cell. 1988; 52:321–328. [PubMed: 3125981]
19. Aguirre-Ghiso JA, Liu D, Mignatti A, Kovalski K, Ossowski L. Urokinase receptor and fibronectin regulate the ERK(MAPK) to p38(MAPK) activity ratios that determine carcinoma cell proliferation or dormancy in vivo. Mol Biol Cell. 2001; 12:863–879. [PubMed: 11294892]
20. Ossowski L, Reich E. Experimental model for quantitative study of metastasis. Cancer Res. 1980; 40:2300–2309. [PubMed: 7190062]
21. Aguirre-Ghiso JA, Ossowski L, Rosenbaum SK. Green fluorescent protein tagging of extracellular signal-regulated kinase and p38 pathways reveals novel dynamics of pathway activation during primary and metastatic growth. Cancer Res. 2004; 64:7336–7345. [PubMed: 15492254]
22. Alonso DF, et al. Characterization of F3II, a sarcomatoid mammary carcinoma cell line originated from a clonal subpopulation of a mouse adenocarcinoma. J Surg Oncol. 1996; 62:288–297. [PubMed: 8691844]
23. Aslakson CJ, Miller FR. Selective events in the metastatic process defined by analysis of the sequential dissemination of subpopulations of a mouse mammary tumor. Cancer Res. 1992; 52:1399–1405. [PubMed: 1540948]
24. Aguirre-Ghiso JA, Estrada Y, Liu D, Ossowski L. ERK(MAPK) activity as a determinant of tumor growth and dormancy; regulation by p38(SAPK). Cancer Res. 2003; 63:1684–1695. [PubMed: 12670923]
25. Kim J, Yu W, Kovalski K, Ossowski L. Requirement for specific proteases in cancer cell intravasation as revealed by a novel semiquantitative PCR-based assay. Cell. 1998; 94:353–362. [PubMed: 9708737]
26. Ossowski L, Reich E. Antibodies to plasminogen activator inhibit human tumor metastasis. Cell. 1983; 35:611–619. [PubMed: 6418388]
27. Henckaerts E, Langer JC, Orenstein J, Snoeck H-W. The Positive Regulatory Effect of TGF-β2 on Primitive Murine Hemopoietic Stem and Progenitor Cells Is Dependent on Age Genetic

Background, and Serum Factors. The Journal of Immunology. 2004; 173:2486–2493. [PubMed: 15294963]

28. Gao H, et al. The BMP Inhibitor Coco Reactivates Breast Cancer Cells at Lung Metastatic Sites. Cell. 2012; 150:764–779. [PubMed: 22901808]
29. Lopez-Casillas F, Wrana JL, Massague J. Betaglycan presents ligand to the TGF beta signaling receptor. Cell. 1993; 73:1435–1444. [PubMed: 8391934]
30. Criswell TL, Dumont N, Barnett JV, Arteaga CL. Knockdown of the transforming growth factor-beta type III receptor impairs motility and invasion of metastatic cancer cells. Cancer Res. 2008; 68:7304–7312. [PubMed: 18794117]
31. Siegel PM, Massague J. Cytostatic and apoptotic actions of TGF-beta in homeostasis and cancer. Nat Rev Cancer. 2003; 3:807–821. [PubMed: 14557817]
32. Gath HJ, Brakenhoff RH. Minimal Residual Disease in Head and Neck Cancer. Cancer and Metastasis Reviews. 1999; 18:109–126. [PubMed: 10505550]
33. Aguirre-Ghiso JA, Bragado P, Sosa MS. Metastasis awakening: targeting dormant cancer. Nat Med. 2013; 19:276–277. [PubMed: 23467238]
34. Kobayashi A, et al. Bone morphogenetic protein 7 in dormancy and metastasis of prostate cancer stem-like cells in bone. The Journal of Experimental Medicine. 2011; 208:2641–2655. [PubMed: 22124112]
35. Shiozawa Y, et al. GAS6/AXL axis regulates prostate cancer invasion, proliferation, and survival in the bone marrow niche. Neoplasia. 2010; 12:116–127. [PubMed: 20126470]
36. Padua D, et al. TGFbeta primes breast tumors for lung metastasis seeding through angiopoietin-like 4. Cell. 2008; 133:66–77. [PubMed: 18394990]
37. Turley RS, et al. The type III transforming growth factor-beta receptor as a novel tumor suppressor gene in prostate cancer. Cancer Res. 2007; 67:1090–1098. [PubMed: 17283142]
38. Cheifetz S, et al. The transforming growth factor-beta system, a complex pattern of cross-reactive ligands and receptors. Cell. 1987; 48:409–415. [PubMed: 2879635]
39. Cheifetz S, et al. Distinct transforming growth factor-beta (TGF-beta) receptor subsets as determinants of cellular responsiveness to three TGF-beta isoforms. J Biol Chem. 1990; 265:20533–20538. [PubMed: 1700790]
40. Brown CB, Boyer AS, Runyan RB, Barnett JV. Requirement of type III TGF-beta receptor for endocardial cell transformation in the heart. Science. 1999; 283:2080–2082. [PubMed: 10092230]
41. You HJ, Bruinsma MW, How T, Ostrander JH, Blobe GC. The type III TGF-beta receptor signals through both Smad3 and the p38 MAP kinase pathways to contribute to inhibition of cell proliferation. Carcinogenesis. 2007; 28:2491–2500. [PubMed: 17768179]
42. Ajiboye S, Sissung TM, Sharifi N, Figg WD. More than an accessory: implications of type III transforming growth factor-beta receptor loss in prostate cancer. BJU Int. 2010; 105:913–916. [PubMed: 20067462]
43. Dong M, et al. The type III TGF-beta receptor suppresses breast cancer progression. J Clin Invest. 2007; 117:206–217. [PubMed: 17160136]
44. Sun CK, Chua MS, He J, So SK. Suppression of glypican 3 inhibits growth of hepatocellular carcinoma cells through up-regulation of TGF-beta2. Neoplasia. 2011; 13:735–747. [PubMed: 21847365]
45. Yamazaki S, et al. TGF-beta as a candidate bone marrow niche signal to induce hematopoietic stem cell hibernation. Blood. 2009; 113:1250–1256. [PubMed: 18945958]
46. Sharifi N, Hurt EM, Kawasaki BT, Farrar WL. TGFBR3 loss and consequences in prostate cancer. Prostate. 2007; 67:301–311. [PubMed: 17192875]
47. Morrissey C, Vessella RL. The role of tumor microenvironment in prostate cancer bone metastasis. J Cell Biochem. 2007; 101:873–886. [PubMed: 17387734]
48. Ghajar CM, et al. The perivascular niche regulates breast tumour dormancy. Nat Cell Biol. 2013
49. Ossowski L, Russo H, Gartner M, Wilson EL. Growth of a human carcinoma (HEp3) in nude mice: rapid and efficient metastasis. J Cell Physiol. 1987; 133:288–296. [PubMed: 3119604]
50. Ranganathan AC, Zhang L, Adam AP, Aguirre-Ghiso JA. Functional coupling of p38-induced up-regulation of BiP and activation of RNA-dependent protein kinase-like endoplasmic reticulum

kinase to drug resistance of dormant carcinoma cells. Cancer Res. 2006; 66:1702–1711. [PubMed: 16452230]

51. Deryugina EI, et al. Unexpected effect of matrix metalloproteinase down-regulation on vascular intravasation and metastasis of human fibrosarcoma cells selected in vivo for high rates of dissemination. Cancer Res. 2005; 65:10959–10969. [PubMed: 16322244]
52. Zijlstra A, Lewis J, Degryse B, Stuhlmann H, Quigley JP. The inhibition of tumor cell intravasation and subsequent metastasis via regulation of in vivo tumor cell motility by the tetraspanin CD151. Cancer Cell. 2008; 13:221–234. [PubMed: 18328426]
53. Dontu G, et al. In vitro propagation and transcriptional profiling of human mammary stem/progenitor cells. Genes Dev. 2003; 17:1253–1270. [PubMed: 12756227]

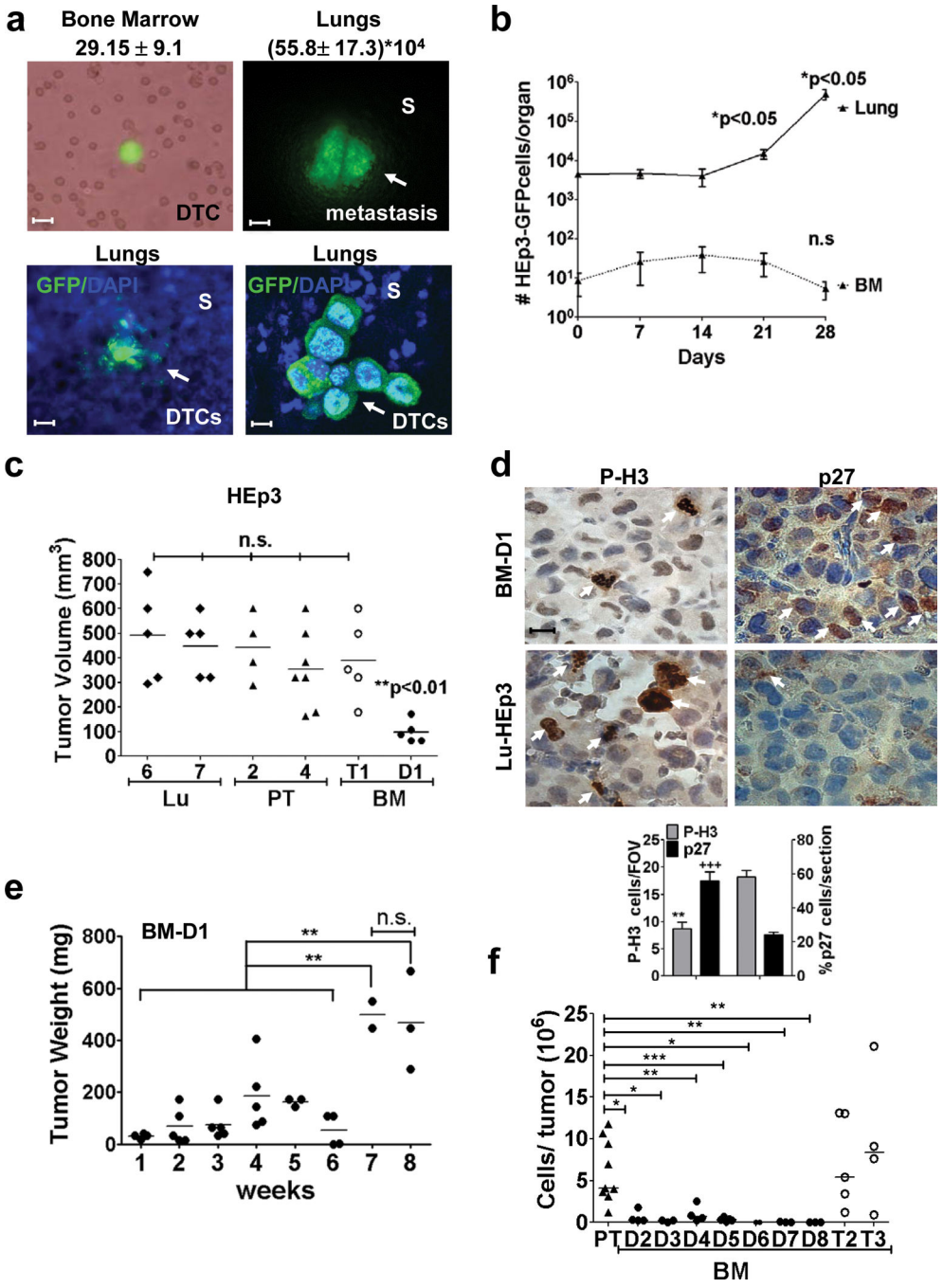

Figure 1. Growth behaviour of BM- and lung-derived DTCs

(**a**) Phase contrast and GFP channel images of a single DTC in a BM flush (upper left panel) and a lung metastasis (upper right panel) 3 wks after primary tumour surgery. Scale bar: 40 μm (BM), 400 μm (lung). S= stroma. Lower left panel: fluorescence images of lungs stroma and a micro-metastasis in a freshly resected lung. Lower right panel: laser scanning confocal image of a DTC cluster in lung. Scale bar: 160 μm (left), 20 μm (right). n=16 (BM), 35 (LU) mice. (**b**) Number of HEp3-GFP DTCs found in lungs and BM after primary tumour surgery (n=5 mice / time / condition). (**c**) Tumour volume of primary tumour- (PT-HEp3), lung-

(Lu-HEp3) and BM-DTC-derived cell lines (BM-HEp3) from mice, after 1 week on CAM. BM-**T**1= tumorigenic *in vivo*, BM-**D**1=dormant*in vivo*. (n=5 (Lu6), 5 (Lu7), 4 (PT-2), 7 (PT-4), 5 (BM-T1), 5 (BM-D1) tumours). (**d**) Phospho-Histone3 (P-H3) (left column) and p27 (right column) staining in BM-D1 (upper panels) tumour nodules and Lu-7 (lower panels) tumours grown on CAMs. Scale bar: 40 μm. Arrows = positive cells. Lower panel: quantification of P-H3 and p27 positive cells (n=100 cells assessed/section. 15 sections assessed from 3 different tumour/ condition). FOV = field of view. (**e**) Weight of BM-D1 tumour nodules on CAMs. BM-D1 cells were inoculated on CAM (5×10^5 cells/animal) and transplanted into a new CAM every week (n=3 (week1), 5 (week2), 5 (week 3), 5 (week 4), 3 (week 5), 4 (week 6), 2 (week 7), 3 (week 8) tumours/ time point). (**f**) Number of tumour cells / CAM nodule produced by primary tumour- (PT-HEp3) and BM-DTC cell lines (BM-HEp3) derived from avian after 1 week on CAM (n=4 (BM-D2), 3 (BM-D3), 4 (BM-D4), 10 (PT), 5 (BM-D5), 5 (BM-T2), 4 (BM-T3), 2 (BM-D6), 3 (BM-D7), 3 (BM-D8) tumours). See supplementary table S4 for statistic source data. Data in **a, b and d**, represent mean ± s.e.m. In **b** and **d**, *p<0.05, **p<0.01 and +++p<0.001 by Mann Whitney test. In **c** and **f** *p<0.05, **p<0.01 and ***p<0.001 by One-way ANOVA-Bonferroni's multiple comparison test and in **e** **p<0.01 by Unpaired t test.

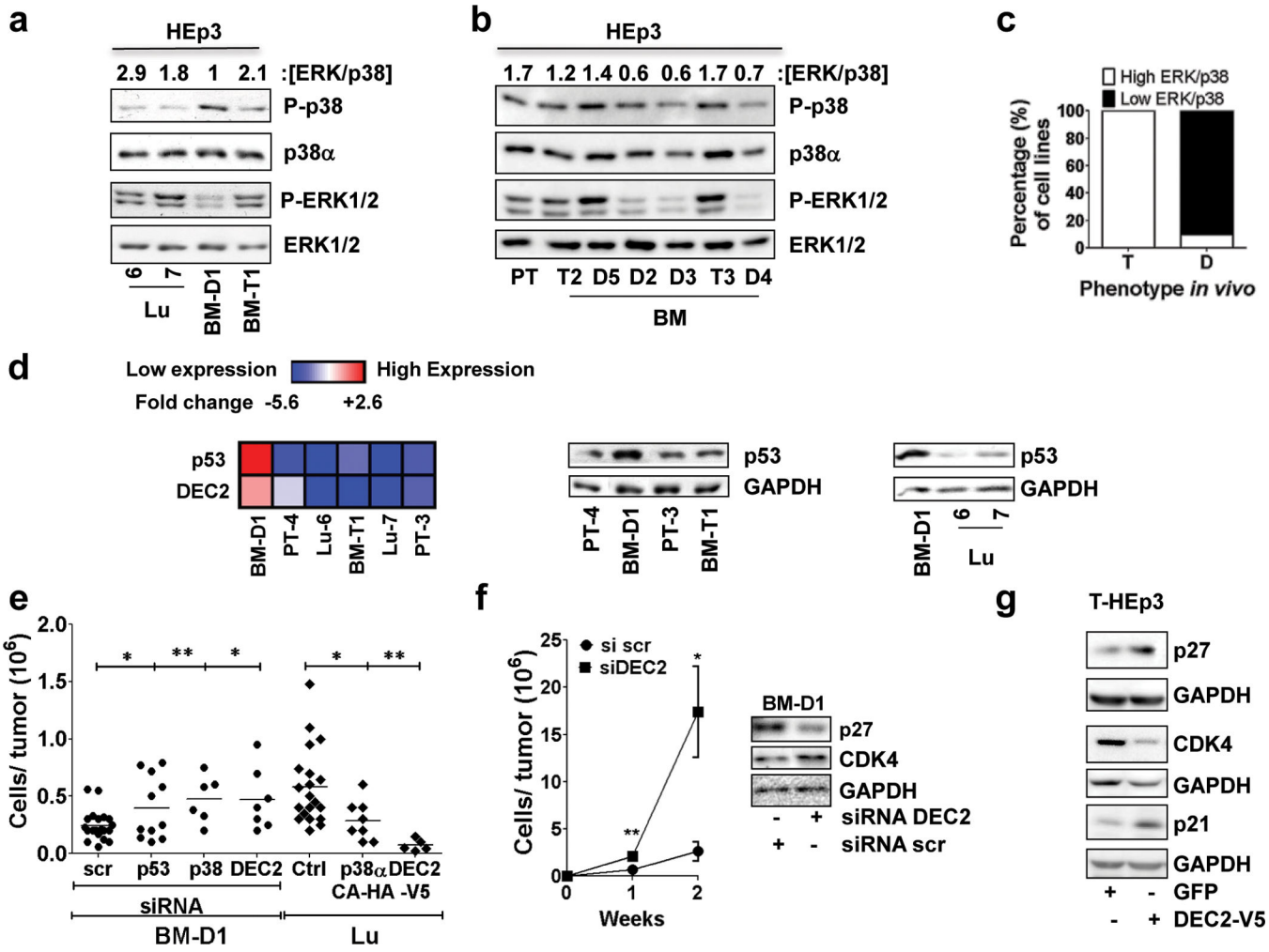

Figure 2. Signalling pathways and genes regulating dormancy of BM-HEp3 Cells

(a–b) Lysates from the indicated DTC-derived cell lines from murine (**a**) and avian microenvironments (**b**) were probed by immunoblot (IB) for the indicated antigens. Numbers on top of blots = [ERK/p38] ratio quantification (see Methods). (**c**) Graph showing percentage of cell lines with high or low ERK/p38 ratio and their phenotype*in vivo*. (**d**) Left panel: Heat map showing DEC2 and p53 mRNA expression in the indicated cell lines after 24h in culture. Scale = log2 fold change and upregulation of mRNAs (red) was significant ($p<0.05$). Middle and right panels: IB for p53 and GAPDH in the indicated cell lines after 24h in culture. (**e**) BM-D1 cells transfected with either scrambled (scr), p53, p38α or DEC2 siRNAs or Lu-HEp3 cells transfected with empty vector (Ctrl) or a constitutively active p38α construct (p38α-CA-HA) or a DEC2-V5 construct were inoculated *in vivo* (5×10^5 BM-D1 cells / CAM and 2.5×10^5 lu-7 cells / CAM) for 5 days. The graph represents the number of cells per tumour nodule (n=18 (scr), 12 (p53), 6 (p38), 7 (dec2), 20 (Ctrl), 7 (p38CA-HA), 5 (DEC2-V5) tumours per condition). *$p<0.05$ and **$p<0.01$ by one-way ANOVA-Bonferroni's multiple comparison test. (**f**) Growth of BM-D1 cells on CAM after RNAi to DEC2 for two weeks *in vivo*. BM-D1 cells transfected with scrambled (scr) or DEC2 siRNA were inoculate in CAMs (5×10^5 BM-D1 cells / CAM). One week after the

tumour nodules were mince, cells/tumour nodule were quantified, transfected again with either scrambled or DEC2 siRNAs and reinoculated again *in vivo*. Graph= mean number of cells / tumour nodule ± s.e.m. (n=4-Si scr week1, 5 Si DEC2 week1, 3-Si scr week2, 5 Si DEC2 week2 tumours per condition). See supplementary table S4 for statistic source data. *p<0.05 and **p<0.01 by Mann Whitney Test. Right panel: p27 and CDK4 expression in BM-D1 cell lines after DEC2 inhibition with siRNAs. Scr=scrambled. (**g**) p27, p21 and CDK4 immunoblot in T-HEp3 cells transfected with either a GFP or a DEC2-V5 construct for 24h.

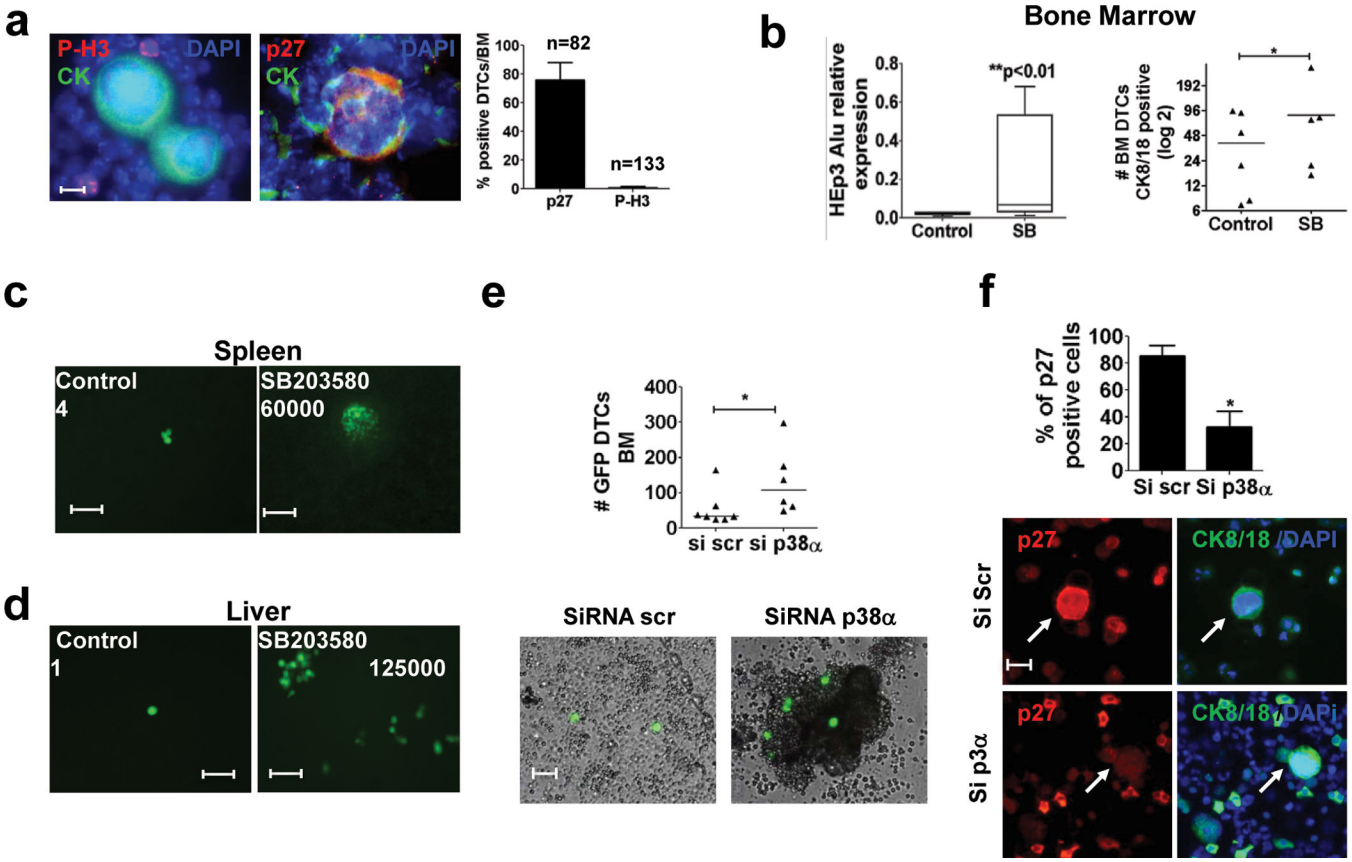

Figure 3. Systemic p38α/β inhibition affects HNSCC DTC behaviour in growth restrictive microenvironments

(**a**) Representative images of Cytokeratin 8/18 (CK), P-H3 (left) and p27 (right) staining in solitary BM DTCs in BM cytospins. Scale bar: 10 μm. Right Graph: percentage of p27 and P-H3 positive DTCs / BM flush, Numbers on top = n for scored DTCs. 6 BM flushes/ 3 independent experiments were assessed (**b**) Quantification of BM-DTCs in mice treated with DMSO (control) or SB203580 (SB) (10 mg/kg every 48 hrs) for 4 weeks. Left Graph: *Alu* qPCR quantification of BM DTCs shows the human *Alu* genomic signal normalized to genomic mouse GAPDH (n=6 (control), 15 (SB) DNA samples were assessed over 3 independent experiments) (see methods for details). Right Graph: quantification of CK positive cells in mice BM cytospins (n=6 BM samples / condition were assessed over 2 independent experiments). *p<0.05 by wilcoxon signed rank test. (**c–d**) Live imaging of HEp3-GFP DTCs, micro and macrometastasis in spleen (**c**) and liver (**d**) of control (scale bar: 80μm) and SB203580 treated mice (Spleen, scale bar: 400μm and liver, scale bar: 80μm). Numbers= GFP positive cells per organ. (**e**) Quantification of BM-DTCs in chicken embryos' BM flushes 5 days after inoculation of T-HEp3-GFP cells transfected with either scrambled (si scr) or p38α (si p38α) siRNAs. (n=7 (si Scr), 6 (sip38) BM samples were assessed over 2 independent experiments). Lower panels: representative fluorescence intravital images of BM DTCs in chicken embryo BM flushes. Scale bar: 160μm. (**f**) Graph: percentage of p27 positive cells / BM flush (n=3 BM flushes were assessed over 2 independent experiments). Lower Panels: representative images of CK (right column) and p27 (left column) staining in solitary BM DTCs in chicken embryos BMs 5 days after

inoculation of T-HEp3-GFP cells transfected with scrambled (scr) (upper row) or p38α (lower row) siRNA. Scale bar=40μM. Data in **a, b and f**, represent mean ± s.e.m. In **b (left graph)**, **e** and **f**, *p<0.05, **p<0.01 by Mann Whitney test.

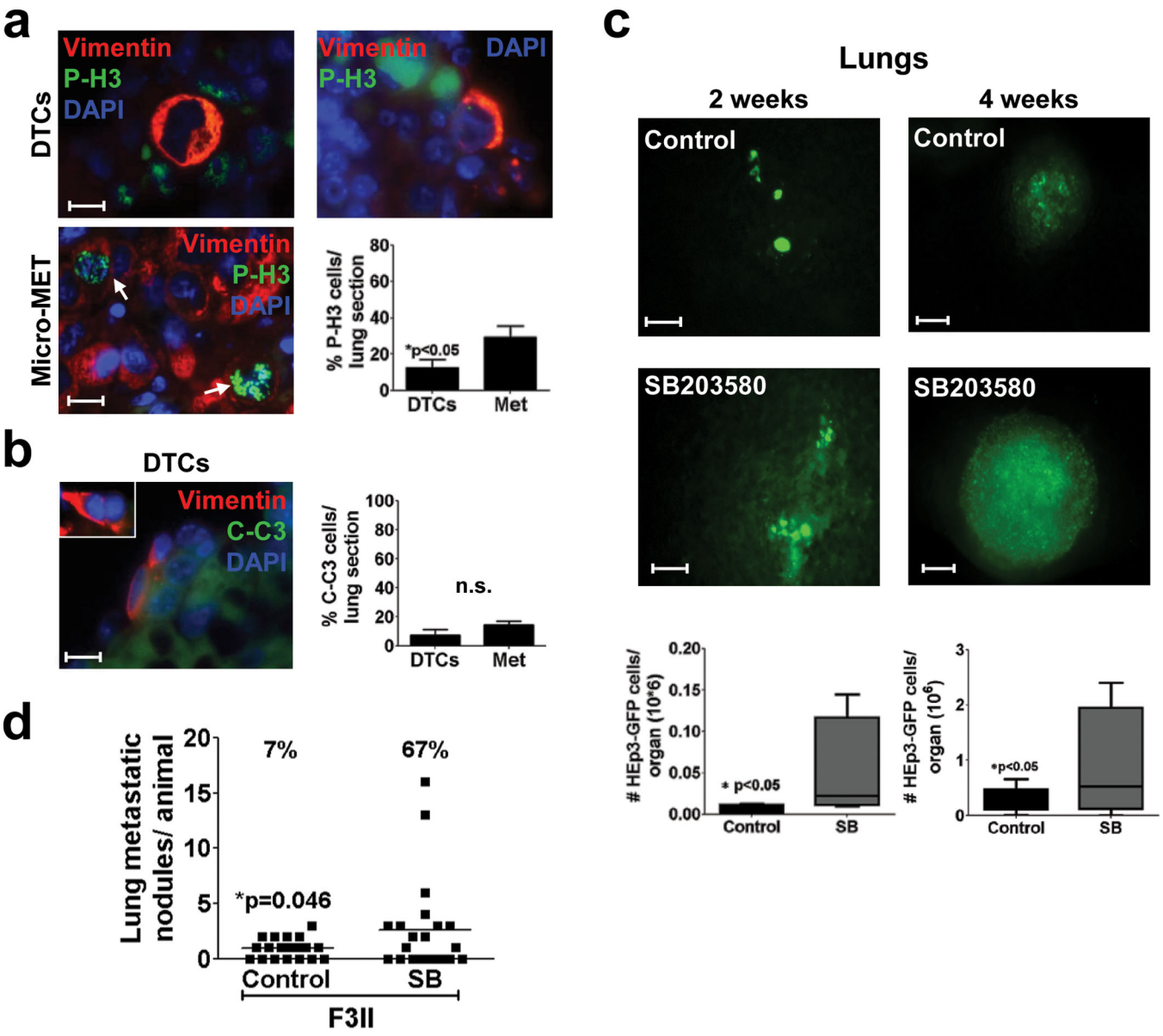

Figure 4. Systemic p38α/β inhibition interrupts DTC dormancy in the lungs

(**a–b**) Representative images of P-H3 and Vimentin (**a**) or Caspase 3 (C–C3) and Vimentin (**b**) staining in lung DTCs (upper panels, scale bar: 20 μm) and lung micro-metastases (micro-MET – **a** only) 4 weeks after surgery (scale bar: 40 μm (Micro-MET (**a**), inset (**b**)). Arrows: marker positive cells. Graphs: % of P-H3 (**a**) or C-C3 (**b**) positive cells per lung section, mean ± s.e.m. of three different lungs, 5 sections per lung (n=45 (DTCs), n=416 (Met) DTCs per lungs section (**a**), n=36 (DTCs) (**b**)). *p<0.05 (**a**) and non significant (n.s.) (**b**) by Mann Whitney Test. (**c**) Representative lung images containing HEp3-GFP DTCs or metastasis (scale bars: 80 μm, left column and 400 μm right column) after surgery and control or SB203580 (SB) (10 mg/kg every 48 hrs) treatment for 2 and 4 weeks. Lower Graphs: quantification of HEp3-GFP cells in whole lung suspensions. (n=5 (Left graph) and 4 (right graph) lungs per condition). See Supplementary table S4 for the statistic source data

of the right graph. *p<0.05 by Mann Whitney Test. (**d**) Number of lung F3II breast cancer macro-metastasis / lung in mice treated with DMSO (control) or SB203580 (SB). Top numbers: prevalence (%) of mice with more than 3 metastatic nodules per lung. n=25 mice, *p=0.046 by Mann Whitney Test.

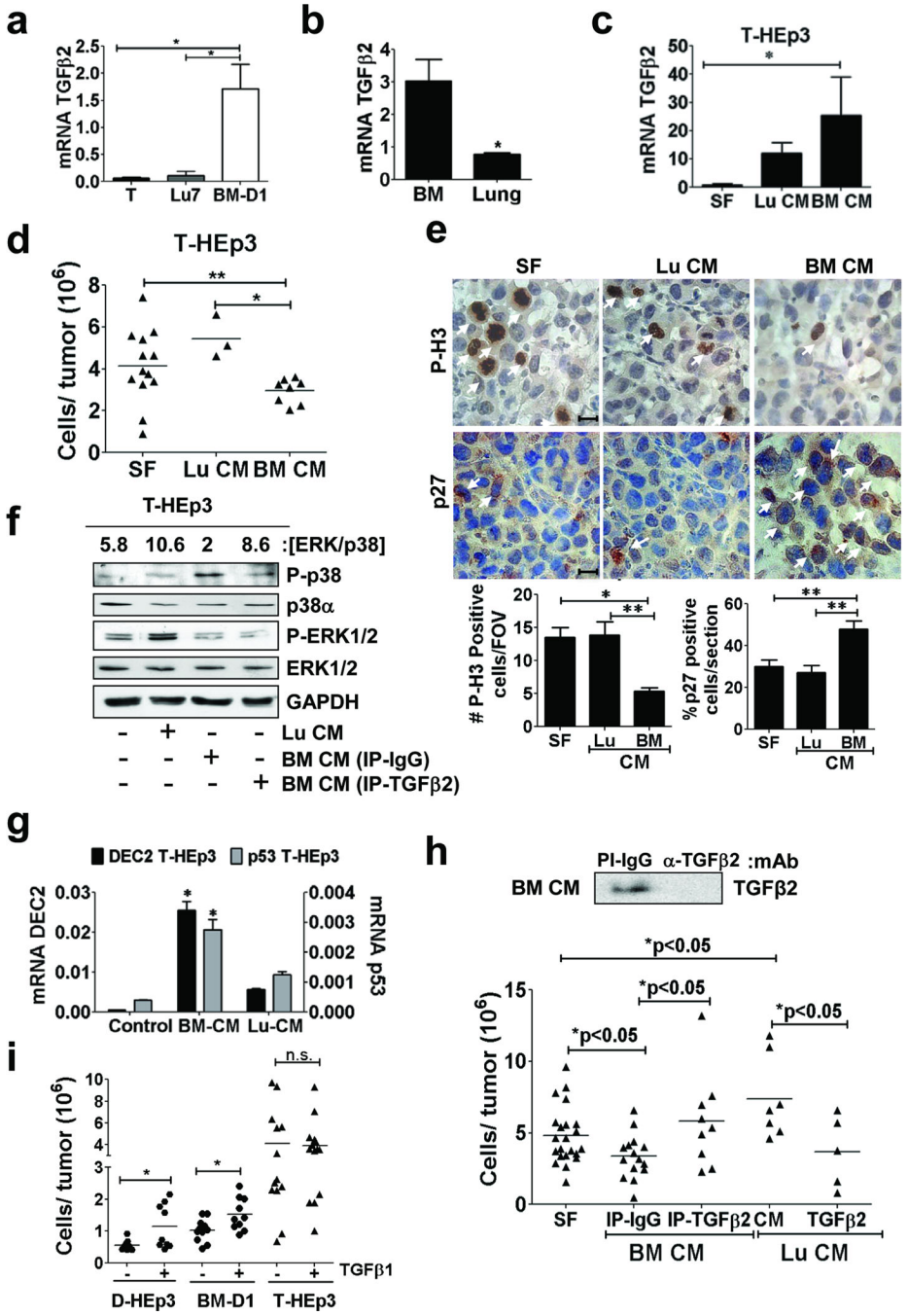

Figure 5. Role of TGFβ2 in dormant HEp3 DTCs

(a–b) Q-PCR analysis of TGFβ2 mRNA levels in the indicated cells cultured in serum-free media for 24h (**a**) in BM and lungs mice organs (**b**) (n=6 RNA samples per condition were assessed over 3 independent experiments). (**c**) Q-PCR for TGFβ2 mRNA in T-HEp3 cells treated with serum-free media (SF) or conditioned media (CM) from lung (Lu CM) or BM (BM CM) (24h). (n=6 RNA samples were assessed over 3 independent experiments). (**d**) Growth after 5 days of T-HEp3 cells on CAMs ($2*10^5$cell/CAM) pre-treated in culture for 24h and then on the CAM every day with SF, BM CM or Lu CM (n=11 (SF), 3 (lu CM), 8

(BM CM) tumour nodules per condition). (**e**) Immunohistochemistry (IHC) for P-H3 (upper row) and p27 (lower row) in T-HEp3 tumour nodule sections after treatment with SF (left column), Lu CM (middle column) or BM CM (right column) for 5 days *in vivo*, scale bar: 40 μm. Arrows: marker-positive cells. Lower graphs: Quantification of P-H3 (left) and p27 (right) positive cells (n=100 cells assessed/section. 15 sections assessed from 3 different tumour/ condition). (**f**) Detection of the indicated antigens in lysates of T-HEp3 cells treated with, SF, Lu CM or BM CM control (IP-IgG) or TGFβ2 immunodepleted (IP- TGFβ2) for 24h. Top numbers: [ERK/p38] ratio quantification. (**g**) Q-PCR for p53 and DEC2 mRNA in T-HEp3 cells treated as in **c** (n=6 RNA samples were assessed over 3 independent experiments). (**h**) Top panel: IB against TGFβ2 in the BM CM after IgG or anti-TGFβ2 immunodepletion. Lower panel: Tumour growth of T-HEp3 cells treated with full or TGFβ2-immunodepleted BM CM or with Lu CM supplemented with PBS (CM) or with 2 ng/ml TGFβ2 (n=22 (SF), 15 (IP-IgG), 8 (IP-TGFb2), 7 (lu CM), 5 (Lu-Cm TGFB2) tumours per condition). (**i**) Effect of TGFβ1 (2 ng/ml) on T-HEp3 and dormant D-HEp3 and BM-D1 tumour growth on CAMs for 5 days *in vivo* (n=6 (DHEp3-TGFb1), 9 (DHEp3+TGFb1), 10 (BM-D1-TGFb1), 10 (BM-D1+TGFb1), 13 (THEp3-TGFb1), 11 tumours per condition). Data in **a, b, c, e and g**, represent mean ± s.e.m. In **a, b, c, e** and **g**, *p<0.05, **p<0.01 by Mann Whitney test. In **d, h and i** *p<0.05, **p<0.01 by One-way ANOVA-Bonferroni's multiple comparison test.

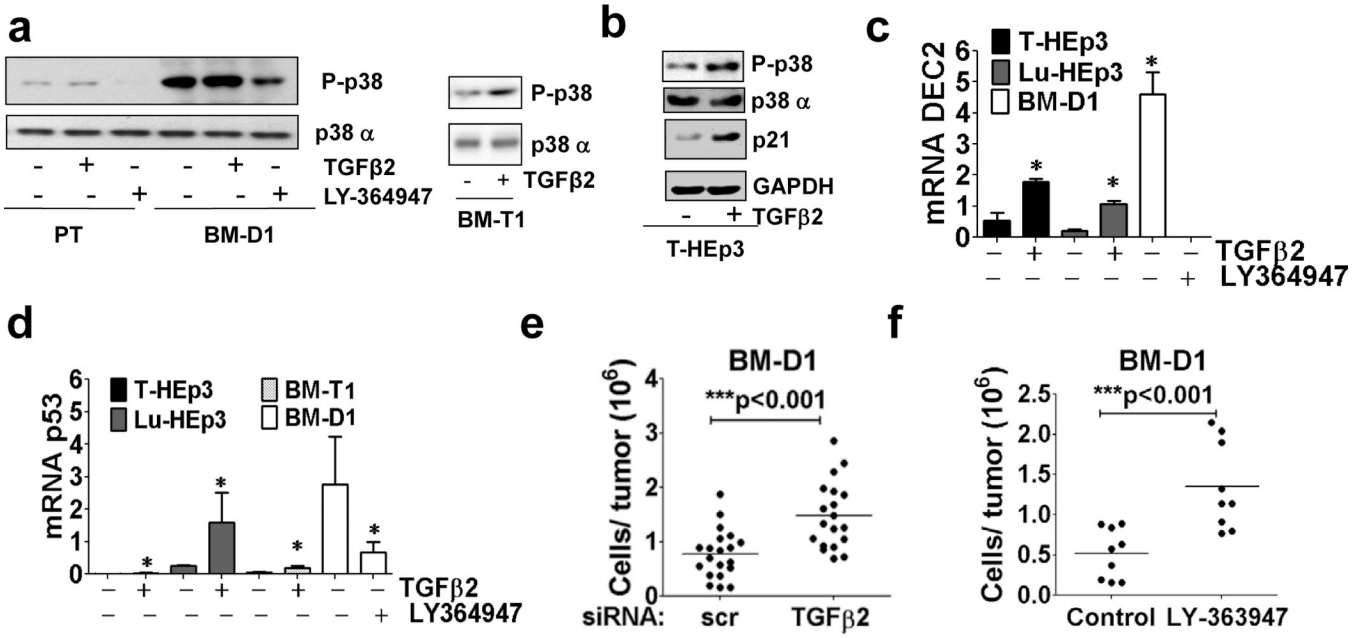

Figure 6. Effect of TGFβ signalling on dormancy and self-renewal markers

(a) IB for the indicated antigens on PT-HEp3 (PT), BM-D1 and BM-T1 cell lysates after TGFβ2 (2 ng/ml) or TGFβRI inhibitor (LY-364947, 5 μM) treatment for 24 h in SF media. (**b**) IB for the indicated antigens on T-HEp3 cell lysates after treatment with TGFβ2 (2 ng/ml) for 24 h in SF media. (**c–d**) QPCR measured DEC2 (**c**) and p53 (**d**) mRNA levels in the indicated cells after treatment with 2 ng/ml TGFβ2 or LY-364947, 5 μM for 24 h in SF media (n=6 RNA samples were assessed over 3 independent experiments). (**e**) BM-D1 growth on CAMs for 4 days after TGFβ2 knockdown. BM-D1 cells were transfected with either scrambled (scr) or TGFβ2 siRNA and inoculated onto CAMs ($5*10^5$ cells/CAM) for 4 days (n=20 (scr), 19 (TGFβ2) tumours per condition). (**f**) BM-D1 growth on CAMs for 4 days after TGFβRI inhibition with LY364947 (5μM). BM-D1 cells were pre-treated with TGFβRI inhibitor (LY-364947, 5 μM) for 24 h in SF media and then inoculated onto CAMs ($5*10^5$ cells/CAM) for 5 days. Tumour nodules were treated with LY-364947 (5 μM) ever day in the CAMs (n=9 tumours per condition). Data in **c and d** represent mean ± s.e.m. In **c, d, e and f** *p<0.05, **p< 0.01, ***p<0.001 by Mann Whitney Test.

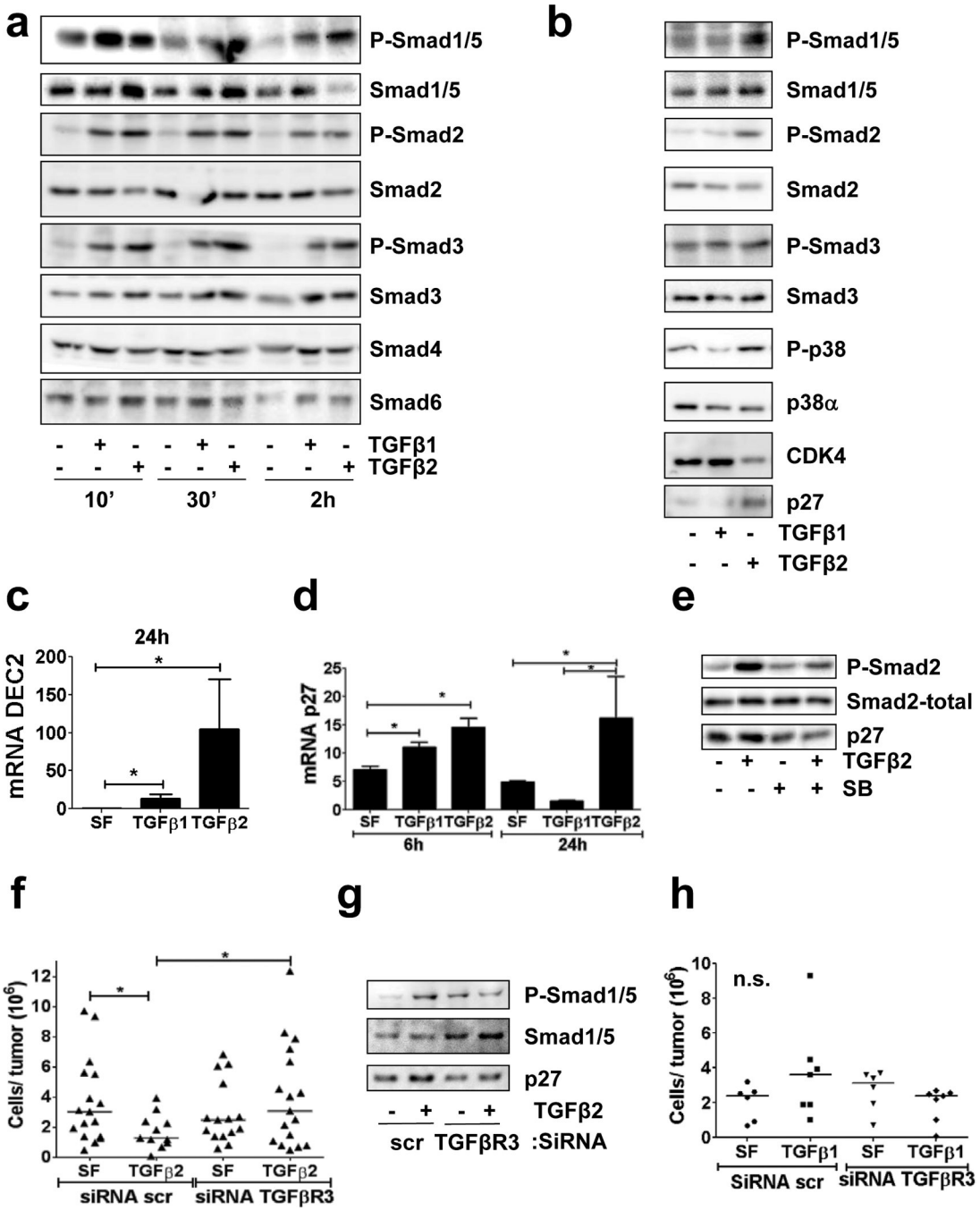

Figure 7. TGFβ2/TGFβ receptor III signalling regulates DTC dormancy

(a–b) IB for the indicated antigens on T-HEp3 cell lysates after treatment with either TGFβ1 or TGFβ2 (5 ng/ml) for 10, 30 min and 2 h (**a**) and 24 h (**b**) in SF media. (**c–d**) QPCR for DEC2 (**c**) and p27 (**d**) mRNA levels in T-HEp3 cells treated with either TGFβ1 or TGFβ2 (5 ng/ml) for 6 (**d**) and 24 h in SF media (n=6 RNA samples were assessed over 3 independent experiments) *p<0.05 by Mann Whitney Test. Error bars denote s.e.m. (**e**) IB for the indicated antigens on cell lysates of T-HEp3 treated with 5 ng/ml TGFβ2 for 24h in SF media with or without SB203580 (SB) (5 μM) (**f**) T-HEp3 tumour growth on CAMs for 4

days of T-HEp3 cells with TGFβR-III knockdown (siRNA TGFRβ3) treated with 5 ng/ml TGFβ2 (n=16 (scr, SF), 11 (scr, TGFb2), 15 (TGFbR3, SF), 17 (TGFbR3, TGFb2)), *p<0.05 by One-way ANOVA-Bonferroni's multiple comparison test. (**g**) IB for the indicated antigens on cell lysates of T-HEp3 treated with TGFβ2 (5 ng/ml) for 24 h in SF media and after TGFβR-III knockdown (siRNA TGFRβ3). (**h**)Tumour growth on CAMs for 4 days after treatment with TGFβ1 (2 ng/ml) in T-HEp3 cells after type III TGFβ receptor knockdown (siTGFβR3) (n=6 (scr, SF), n=7 (scr, TGFb1), n=6 (SiTGFBR3, SF), n=6 (SiTGFBR3, TGFb1)), p=0.3246 by One-way ANOVA-Bonferroni's multiple comparison test.

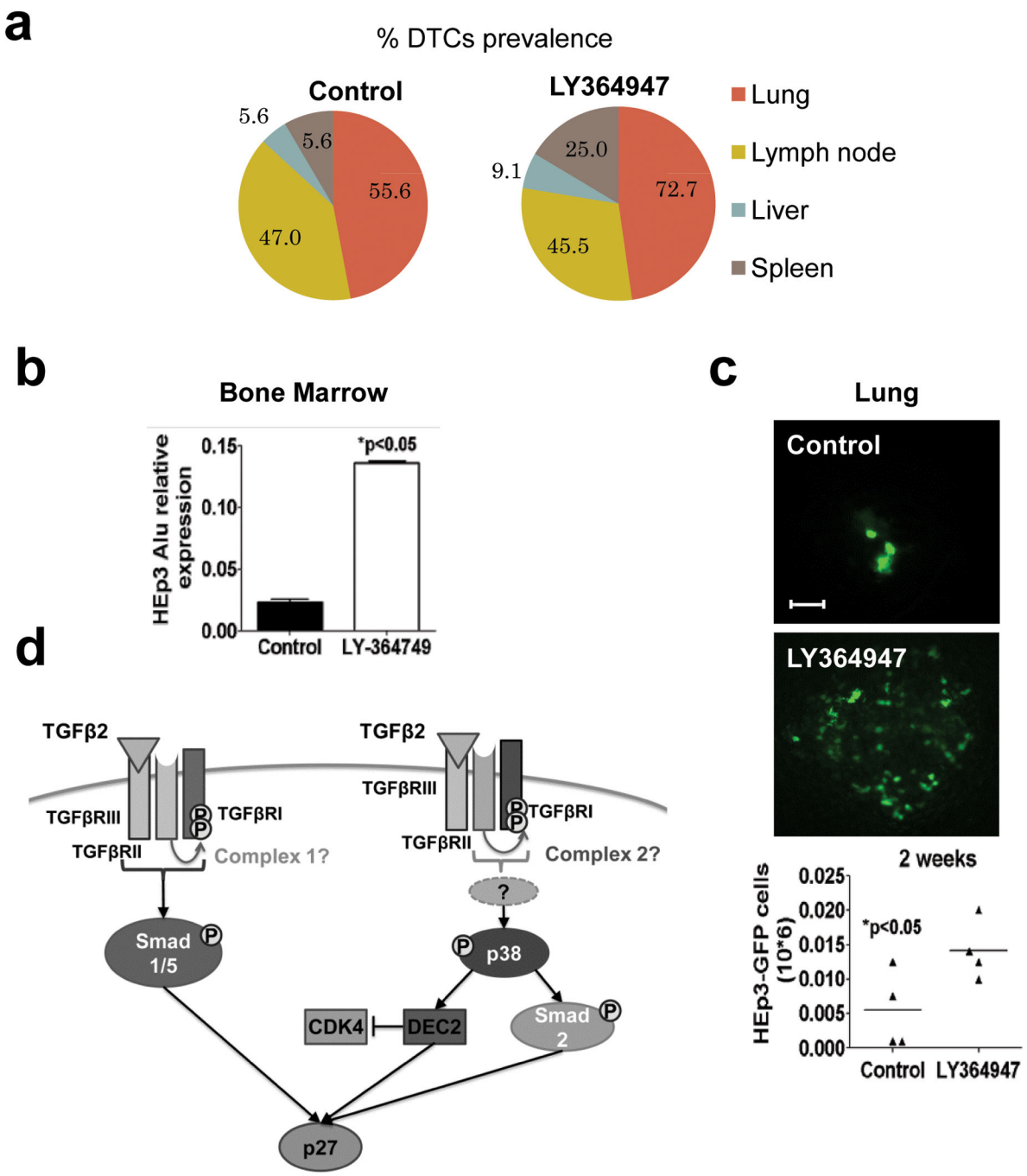

Figure 8. Effect of TGFβRI inhibition on DTC burden

(**a**) Prevalence of HEp3 DTCs (%) per mouse in control (n=20) and LY364947-treated (n=32) animals (2 independent experiments) (**b**) *Alu* qPCR quantification of HEp3 DTCs in BM of mice treated either with DMSO or with LY364947 10 mg/kg every 48 h for 2 weeks. Graph: mean ± s.e.m. of *Alu* amplification signal normalized to mice GAPDH (n=6 DNA samples from 6 different BM samples were assessed over 2 independent experiments), *p<0.05 by Mann Whitney Test. (**c**) Fluorescence images of HEp3-GFP DTCs in mouse lungs, 2 weeks after control (scale bar: 80 μm) and LY364947 treatment (scale bar: 120 μm).

Lower graph: quantification of HEp3-GFP DTCs in lungs of control and LY364947 treated animals. n=4 mice per condition, *p<0.05 by Mann Whitney Test. (**d**) Scheme of the proposed mechanism for TGFβ2-induced dormancy. Binding of TGFβ2 to TGFβ receptor III (TGFβRIII) recruits TGFβ receptor II (TGFβRII) and TGFβ receptor I (TGFβRI) into the complex and activates TGFβ2 signalling which in turn activates Smad1/5 and induces p27. In addition, TGFβ2 also activates p38α in a TGFβRIII independent way. In response to TGFβ2, p38α activates SMAD2 and DEC2, which induces p27 and inhibits CDK4. All these signals integrate and contribute to TGFβ2 induction of quiescence.